

## Petrochemical Characteristics of Neogene and Quaternary Alkali Olivine Basalts from the Western Margin of the Lut Block, Eastern Iran

S. Saadat\*<sup>1</sup>, M. H. Karimpour<sup>2</sup> and Ch. Stern<sup>3</sup>

1. Department of Geological Sciences, University of Colorado, Boulder, CO, USA, and Islamic Azad University, Mashhad Branch, Iran

2. Research Center for ore deposit of Eastern Iran, Ferdowsi University of Mashhad, Iran

3. Department of Geological Sciences, University of Colorado, Boulder, CO, 80309-0399 USA

Received 8 April 2010; accepted 28 September 2010

### Abstract

The Nayband strike-slip fault forms the western margin of the micro-continental Lut block in Eastern Iran. Neogene and Quaternary mafic volcanic rocks collected near Tabas, along the northern part of the fault (NNF; 15 Ma), and further to the south, along the middle part of the fault (MNF; 2 Ma), are within-plate sodic-series alkali olivine basalts with high TiO<sub>2</sub> and up to >16% normative nepheline. Their high MgO, Ni and Cr contents indicate that they crystallized from relatively primitive magmas. Their low La/Nb and Ba/Nb ratios are similar to oceanic island basalts (OIB) and unlike convergent plate boundary arc basalts (IAB). These alkali olivine basalts show enrichment in LREE relative to HREE and limited variation in Sr, Nd and Pb isotopic values which all plot in the range of OIB. Ce/Pb (>39), Nb/U (44-120) and P<sub>2</sub>O<sub>5</sub>/K<sub>2</sub>O (~0.4) ratios suggest that crustal contamination was not significant for MNF basalts. The data may be interpreted as indicating the participation of upwelling mantle asthenosphere and the deeper continental mantle lithosphere in the generation of these basalts. They formed by generally low, but variable degrees of partial mantle melting, which decreased with time from 15 Ma NNF relative to 2 Ma MNF basalts. The small volume of melts that formed the MNF basalts rose to the surface along the deep Nayband strike-slip fault with no interaction with the continental crust. The larger volume of NNF basalts interacted to some degree with the crust and are associated with basaltic andesites and andesites.

**Keywords:** Lut block, Alkali olivine basalt, Isotopic composition, Iran.

### 1. Introduction

The Iranian plateau occurs within a part of the active Alpine-Himalayan orogenic belt, trapped between the Arabian plate to the southwest, the Eurasia plate to the northeast, the Indian oceanic plate to the south, and the Helmand/Afghanistan block to the east (Fig. 1). This plateau includes the Lut block micro-plate, an extremely arid desert region in eastern Iran. The Lut block extends over 900 km in a north-south direction between latitudes 28° to 35°N, and is 200 km wide in an east-west direction between longitudes 57° to 61°E (Fig. 2). The Lut block is bounded on the north by the Dorouneh fault and on the south by the Jazmurian depression and Makran volcanic arc (Figs. 1 and 2). It is separated from the rest of the Iranian plateau by two major belts of north-south right-lateral strike-slip faulting. On the east is the Nehbandan fault and on the west the Nayband fault (Fig. 2). The Lut block is largely covered by Neogene volcanic rocks.

The focus of this paper is primitive mantle-derived Neogene/Quaternary alkali olivine basalts that have erupted along the Nayband fault along the western margin of the Lut block. Geochronological data for these alkaline basalts yield ages of 15 Ma [1] for samples from near Tabas (NNF; Fig. 2), and of 2 to 2.6 Ma [2, 3] for samples from further south, in an area that is called Gandom Beryan (MNF; Fig. 2).

Neogene magmatic activity on the Lut block and elsewhere in Iran is related to arc and back-arc magmatism involving contributions from subducting oceanic slabs, the subcontinental lithospheric and asthenospheric mantle, and the continental crust [4]. The relatively primitive basaltic rocks from the western structural boundary of the Lut block provide a window into the subcontinental mantle below Iran, and the opportunity to determine petrochemical information about this mantle, which is an important first step in understanding all Iranian Neogene magmatism. The aim of this petrological and geochemical study is to characterize the composition of the mantle source region of the Neogene/Quaternary olivine basalts which erupted along the western margin of the Lut block.

\*Corresponding author.

E-mail address (es): Saeed.Saadat@Colorado.edu

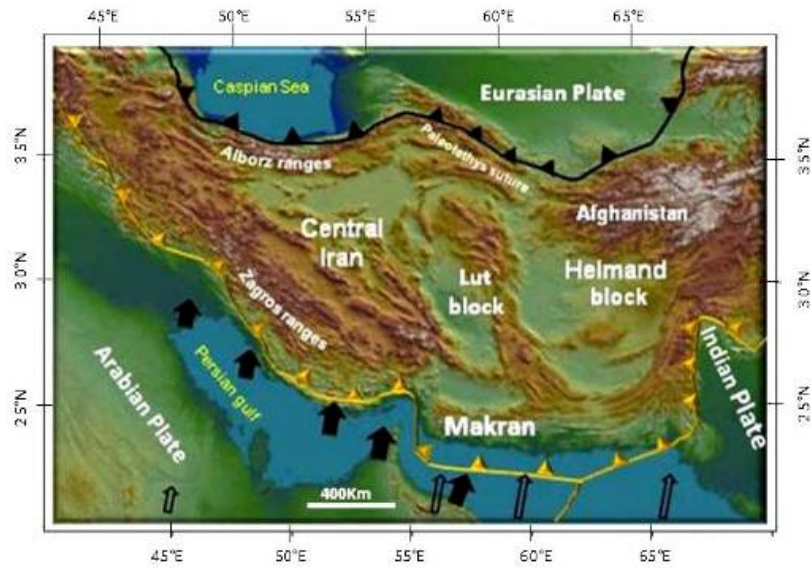


Fig. 1. A general view of the Lut block microplate and its surroundings areas. The orange line represents the plate boundary based on Bird [80] and black line shows the paleo-tethys based on Alavi [81] for northern Iran and from Natal'in and Sengor [82] for northern Afghanistan. The solid black arrows show the direction of convergence based on GPS observation [83]. The open black arrows show the convergence velocity based on NUVEL-1[84].

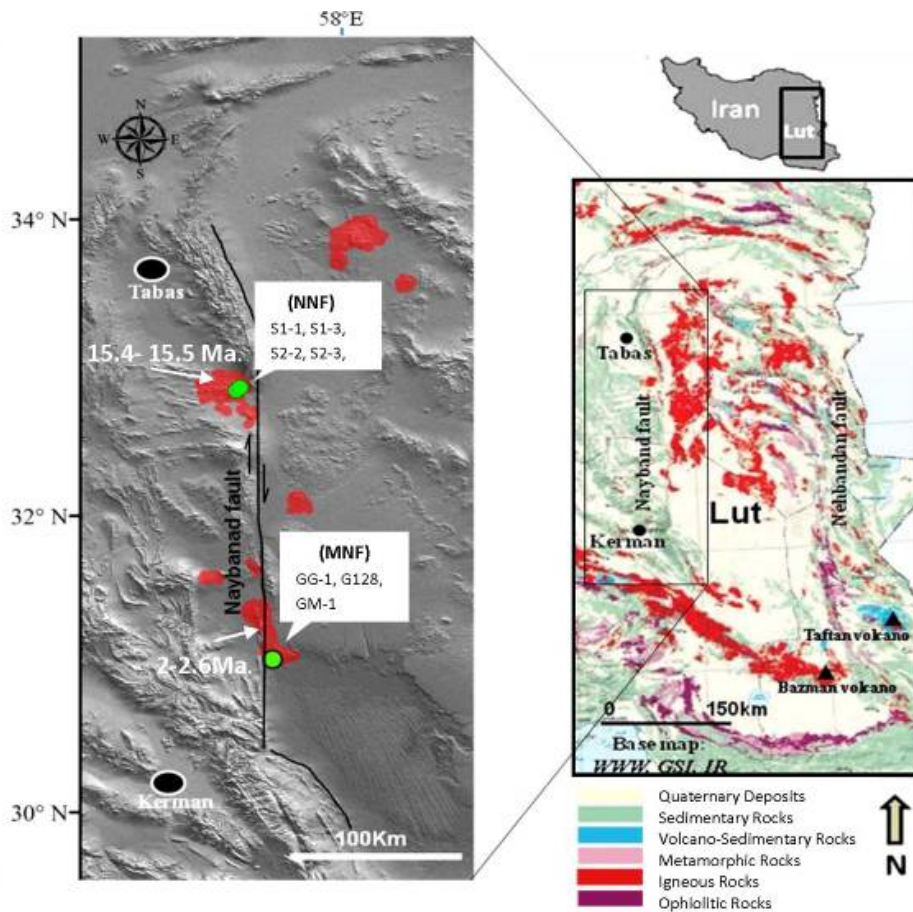


Fig. 2. Location of the Lut block and the study area along the Nayband fault. Distribution of Quaternary basalts are shown with red color, and sample locations from the northern (NNF) and middle part of the fault (MNF) are shown in green circles. Radiogenic age determination from NNF basalts after [1] and from MNF basalts [2-3]

## 2. Geologic setting

According to Stocklin [5], the Lut Block is an irregularly outlined, essentially north-south trending rigid microplate surrounded by the ranges of central and eastern Iran. However, dislocations and other lineaments within the Lut Block, in addition to its internal seismicity and Quaternary volcanic activity, support an argument against the complete rigidity of the Lut block [6].

Although the metamorphic basement of the Lut block has not been dated, Archean [7] to Early Proterozoic [8], Late Proterozoic [9, 10] and late Neoproterozoic to Early Cambrian [11] crystallization ages for granitoids and granitic gneisses have been reported from the crystalline basement elsewhere in Iran. Sedimentary strata in the Lut block are mainly younger than Permian and consist of shallow marine carbonates, shales and sandstones [12]. Continental Neogene sedimentary deposits and Quaternary sand dunes, salt flats and alluvial fans cover large areas of the Lut block (Fig. 2).

Based on very limited geochronologic data, magmatic activity in the Lut block started in the late Jurassic and continued into the Quaternary [13], forming a variety of volcanic and volcanoclastic rocks, as well as subvolcanic stocks, intrusive rocks, and associated mineral deposits. Jung et al. [1] classified Tertiary magmatic rocks in the northern part of the Lut block as basaltic, andesitic, dacitic and rhyolitic, including both extrusive and intrusive forms. The basaltic rocks were subdivided into calc-alkaline, alkaline and very high potassium (shoshonitic) rock series. The andesites, dacites and rhyodacites volcanics were erupted together during the late Cretaceous to the early Neogene [1]. Rhyolite ignimbrites in northern part of the Lut block were erupted repeatedly during this volcanic activity. The oldest of these units is 60-63 Ma and the youngest units indicate K-Ar age around 31 Ma [1]. The Middle Eocene (47 Ma) is distinguished by alkaline and shoshonitic volcanism [14]. Maximum volcanic activity on the Lut block took place at the end of the Eocene. Recent Ar-Ar age dating [15] of one andesitic sample from the Lut block indicates a late Oligocene age (25.1 Ma).

In the southern part of the Lut block there are the two large dormant Taftan and Bazman strato-volcanoes within the Makran arc (Fig. 2). Basalts from the western and eastern part of the Bazman stratovolcano yield ages of 4.6 Ma and 0.6 Ma (K-Ar method; [2]). A sequence about 50 meters thick of tuffs and ignimbrites around Taftan stratovolcano could be as young as 2 Ma [16]. Magmatism in Mt. Taftan is represented by volcanic rocks that vary from basaltic through andesitic to dacitic composition [17].

In addition, Stocklin et al. [18], Arjangravesh [19], Emami [20], Darvishzadeh et al. [21], Rosenberg [22], Khorasani [23], Vosughi Abedini [24],[25], Allahpour

[26], Hashemi [27, 28], Pourlatifi [29] and [30], provide some trace-element geochemistry and very limited isotopic data for other volcanic rocks on the Lut block.

## 3. Analytical techniques

Samples were collected from the sites shown in Figure 2. Both standard petrographic thin sections and polished thin section for electron microprobe were prepared from these samples. Portions of these samples were also powdered for X-Ray fluorescence (XRF) spectrometry analysis for major elements, inductively coupled plasma mass spectrometer (ICP-MS) analysis for trace-elements, and also for determination of the Nd, Sr and Pb isotope compositions by solid source mass-spectrometry techniques described below.

The samples were examined in thin section, using standard techniques of optical mineralogy to determine their textures, mineral contents and rock type. Following visual observation, description and photomicrography, selected thin sections were polished for electron microprobe to determine mineral compositions. This was done by using a 10 micron diamond polishing wheel, followed by a 6 micron polishing wheel and finally a 0.05 alumina powder on a felt pad. Minerals from polished sections were analyzed using the JEOL, JXA-8600 super probe, in the Laboratory for Environmental and Geological Science (University of Colorado at Boulder), with an electron gun accelerating voltage of 15 kV, current range from 17-24 nA and a one micron diameter focused beam. Matrix correction was done by J Armstrong's ZAF correction program using natural mineral standards. Analytical errors are 0.1-1.0 relative percent for major elements and 5-20 percent for minor elements. Detailed discussion of using the electron microprobe as an analytical tool in geology is given by Reed [31].

Rock samples were powdered for whole-rock geochemical analysis. A jaw crusher was used to pulverize samples, which were then powdered to 200 mesh with a tungsten carbide grinder. These rock powders were bottled and sent to the X-Ray Fluorescence (XRF) laboratory in Ferdowsi University of Mashad (Iran), using Philips (X, UniqueII) instrument, for measuring the major elements. Detection limits for Si and Al are 100 and 120 ppm, respectively, and the values reported for other elements are Ca=55 ppm, Fe=15 ppm, K=20 ppm, Mg=30 ppm, Na=35 ppm, Mn=4 ppm and P=135 ppm. Trace-elements and REE were determined by ICP-MS (Inductively Coupled Plasma Mass Spectrometry) using an ELAN DCR-E instrument at the department of the Geological Science, University of Colorado at Boulder. Methods for ICP-MS are similar to those described by Briggs PH. [32]. USGS standards were used as the calibration standard and to

monitor accuracy during ICP-MS analysis. Precision for analytical technique is generally better than 5% at the 95% confidence level.

The isotope lab in the Department of the Geological Science, University of Colorado at Boulder, was used for sample preparation and isotope analyses. Isotopic measurements were carried out on powders of leached whole-rock material. Rock powders for isotopic analysis were generated in a ceramic-lined container.  $^{87}\text{Sr}/^{86}\text{Sr}$  ratios were analyzed using Finnigan-Mat 261 four-collector static mass spectrometer. Replicate analyses of the SRM-987 standard in this mode yielded a mean  $^{87}\text{Sr}/^{86}\text{Sr}$  of  $0.71025 \pm 2$  ( $2\sigma$ ). Measured  $^{87}\text{Sr}/^{86}\text{Sr}$  were corrected to  $\text{SRM-987} = 0.710299 \pm 8$ . Errors are  $2\sigma$  of the mean refer to last two digits of the  $^{87}\text{Sr}/^{86}\text{Sr}$  ratio. The Nd isotopic compositions are reported as  $\epsilon\text{Nd}$  values using a reference  $^{143}\text{Nd}/^{144}\text{Nd}$  ratio of 0.512638. Measured  $^{143}\text{Nd}/^{144}\text{Nd}$  was normalized to  $^{146}\text{Nd}/^{144}\text{Nd} = 0.7219$ . Analyses were dynamic mode, three-collector measurements. Thirty-three measurements of the La Jolla Nd standard during the study period yielded a mean  $^{143}\text{Nd}/^{144}\text{Nd} = 0.511843 \pm 8$  ( $2\sigma$  mean), and as a result static mode  $^{143}\text{Nd}/^{144}\text{Nd}$  ratios determination for unknowns were corrected upwards to agree with the dynamic mode analyses. Details of analytical procedures are given in Farmer et al. [33,34]. Pb isotopic analyses were four-collector static mode measurements. Sixteen measurements of SRM-981 during the study period yielded  $^{208}\text{Pb}/^{204}\text{Pb} = 36.56 \pm 0.03$ ,  $^{207}\text{Pb}/^{204}\text{Pb} = 15.449 \pm 0.008$ ,  $^{206}\text{Pb}/^{204}\text{Pb} = 16.905 \pm 0.007$  ( $2\sigma$  mean). Measured Pb isotope ratios were corrected to SRM-981 values ( $^{208}\text{Pb}/^{204}\text{Pb} = 36.721$ ,  $^{207}\text{Pb}/^{204}\text{Pb} = 15.491$ ,  $^{206}\text{Pb}/^{204}\text{Pb} = 16.937$ ). Total procedural blanks averaged  $\sim 1$  ng for Pb and Sr, and 100 pg for Nd during study period [34]. No age correction was applied to the data because of the young age of the rocks.

## 4. Results

### 4-1. Petrography

The Neogene-Quaternary basalts erupted along the Nayband strike-slip fault are composed of dense black blocky masses. Some of them have a reddish color because of high-temperature oxidizing condition during their eruption. These rocks are in general very fine grained. In some outcrops vesicles with maximum 50 mm diameter are presented. The vesicles are partly filled with zeolites, carbonate and silicate minerals.

These basalts have mainly porphyritic texture with intergranular, subophitic and intersertal groundmass. Photomicrographs of one of these rocks (S3-1) are shown in Figure 3. The phenocrysts in samples from the northern part of the Nayband fault (NNF) comprise 25-30 volume % of the rock, and include olivine (0.5-

1.5 mm in diameter)  $\pm$  clinopyroxene (0.8-1 mm in diameter)  $\pm$  plagioclase (1-1.5 mm in diameter). The phenocrysts of samples from middle part of the Nayband fault (MNF) comprise less than 20 volume % of the rock and include mainly of olivine ( $<0.5$  mm) and clinopyroxene (0.5-2 mm). Plagioclase as a phenocryst is rare in MNF samples. Euhedral and subhedral olivine crystals are surrounded by narrow red-brown rim of iddingsite and in some cases somewhat corroded. In some samples plagioclase laths are embedded in subhedral and anhedral phenocrysts of clinopyroxenes (mainly augite) resulting in subophitic texture. The groundmass generally consists of laths of plagioclase (mainly labradorite), rarely potassium feldspar and small crystals of clinopyroxene. In addition opaque minerals (Ti-magnetite and ilmenite), occasionally glass are present in the groundmass. Minor amounts of secondary calcite occur in some samples.

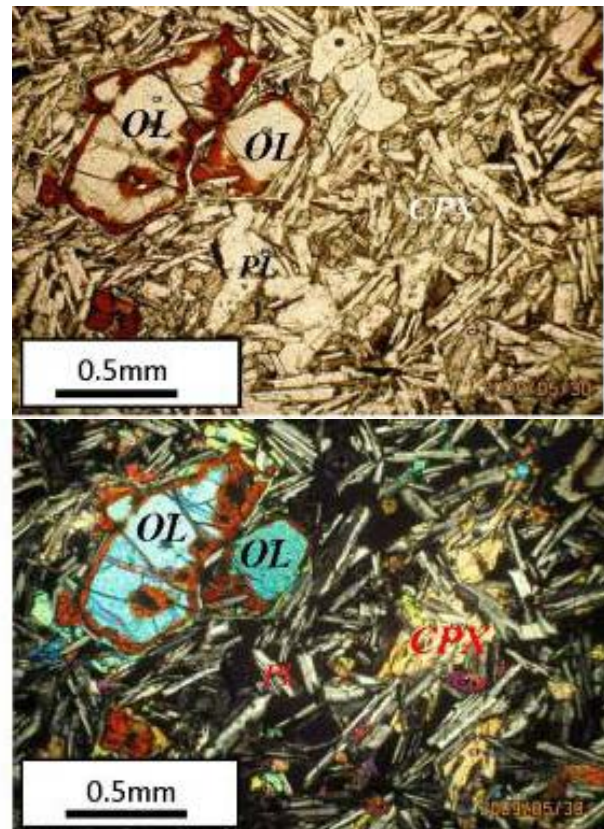


Fig. 3. Photographs show olivine basalts from the west part of the Lut block (NNF, sample S3-1). The phenocrysts (25-30 volume %) are generally magnesian olivine (Fo80), pyroxene (Wo40, En45, Fo15) and plagioclase (An51). The olivine crystals are surrounded by narrow red-brown rim of iddingsite and corroded. Plagioclase laths are embedded in phenocrysts of pyroxenes (subophitic texture). Left photographs are taken in PPL and the right photographs taken under XPL.

## 4-2. Mineral compositions (Mineral chemistry)

### *Olivine*

Compositions of olivine phenocrysts from NNF samples range between Fo68 to Fo84 and from MNF samples range from Fo75 to Fo81. The composition of olivine microliths from MNF samples is around Fo70. Phenocrysts are commonly normally zoned and typically consist of a comparatively large, homogeneous Mg-rich core mantled by a relatively thin, less forsteritic rim.

The measured decrease in Fo content of rims relative to cores commonly less than 10%. Small grains of chromium spinel are present in some olivine phenocrysts from NNF samples.

### *Clinopyroxene*

Clinopyroxene phenocrysts are predominantly augite for both NNF and MNF samples (Wo32-41, En45-47, Fs14-22 and Wo44-48, En39-41, Fs13 respectively). The amount of TiO<sub>2</sub> in clinopyroxenes from the NNF samples range from 0.9% to 1.5 %, whereas this range for MNF samples is higher and varies between 2.1 and 3.7%.

### *Feldspar*

The compositional range of plagioclase from NNF samples is An53-29. This range for MNF samples is almost the same (An51-30). There is no or very weak zoning (core-rim pairs are within the same range of compositions). Rare K-feldspar occurs in the groundmass of some samples.

## 4-3. Whole-rock compositions

### *Major elements*

Table 1 presents the major elements composition of 8 samples of Neogene/Quaternary basalts from the western Lut. None of the samples contain normative quartz, and normative nepheline of the samples varies from absent to greater than 16%. According to silica versus total alkali diagram (Fig. 4), the chemical composition of these rocks are mainly hawaiites, but also include basalts, trachyandesite and tephrite basanite. All samples plot in the alkali field. K<sub>2</sub>O versus Na<sub>2</sub>O (wt. %) and MgO versus TiO<sub>2</sub> diagrams show that these alkali rocks belongs to Na-Series and high-Ti or very close to high-Ti alkali basalts (Fig. 5). These samples show relatively strong positive correlation between CaO versus MgO, whereas SiO<sub>2</sub> contents show strong negative correlations with MgO that are interpreted to result from fractionation of olivine and clinopyroxene (Fig. 5).

### *Compatible and incompatible trace elements*

Trace elements concentrations of western Lut Neogene basalts are presented in Table 2 and their

concentrations are compared with the other continental alkali basalts around the world and also with average of OIB in Table 3. The concentrations of Ni vary from 90 to 111 ppm for samples from northern part of Nayband fault (NNF) and from 152 to 173 ppm for those collected from middle part of this fault (MNF). Chromium in these samples varies between 90-173 ppm and 112-232 ppm, respectively (Table 2). Chromium and nickel both relatively strong positive correlation with MgO (Fig. 5). Nickel is a sensitive indicator of olivine fractionation/accumulation from basaltic magmas because of its large partition coefficient (mineral/melt concentration), and these data suggest decreasing MgO and Ni due in part to olivine fractionation. Decreasing Cr may result from clinopyroxene fractionation.

The geotectonic chemical discrimination diagram, such as those based on Ti-Zr-Y or Nb-Zr-Y, indicate that the samples from this area are similar to other within-plate alkaline basalts (Fig. 6), consistent with their location in the central part of the Iranian Plateau.

Normalized value of trace-element abundances for western Lut Quaternary basalts are presented in Figure 7. These samples are enriched in LREE relative to HREE, a feature typical of alkalic intraplate basalts. Values of (La/Yb)<sub>N</sub> vary from 6.3–11.6 for northern part of Nayband fault (similar to those from Anatolia, Table 3)[35] and from 17.9 to 20.4 for middle part of Nayband fault (similar to Miocene basalts in northwestern Taiwan, Table 3)[36].

Western Lut Neogene basalts are similar to the other continental alkali sodic basalts (Fig. 8) because of their high value of LREE and relative enrichment in high field strength elements (HFSE; La/Nb >0.5), and like most sodic alkaline continental magmas they have trace-element characteristics similar to those of oceanic island basalts [e.g., 37, 38-40]. None of the samples show depletions in Nb relatively to LILE (Ba, Sr). The patterns for NMF group are less enriched in LREE than MNF group and the other alkali basalts listed in Table 3, but the abundances of Ti, Y and Yb in both groups are almost the same and are very similar to average OIB (Fig.7)[41]. Other characteristics, such as low La/Nb (0.5-0.65) and Ba/Nb ratios (6-13) are similar to oceanic island basalts (OIB) and unlike convergent plate boundary arc basalts (Fig. 8 and 9). Strontium doesn't show negative anomalies suggesting that it behaved incompatibly for these lavas.

(a) - (c)

These samples have average Ce/Pb=17 for NNF and more than 39 for MNF. Nb/U ratio is varies from 43 to 69 for NNF samples and from 44 to 123 for MNF samples (Fig. 10), relatively similar to those basalts derived from OIB-like sources unaffected by crustal contamination (Ce/ Pb~25±5, Nb/ U~47±10, 41, Ce/ Pb~25±5, Nb/ U~47±10, [41-43]).

Table 1. Major elements composition of western Lut Quaternary basalts

Location	NNF					MNF		
Sample No.	S1-1	S1-3	S2-2	S2-3	S3-1	GM-1	Gg-1	G128
Rock type	T. Ande.	Basalt	Haw.	Basalt	Haw.	Haw.	Haw.	Ba. T
SiO <sub>2</sub>	52.7	51.2	51.6	49	49.9	46.2	46.2	45.6
TiO <sub>2</sub>	2.5	2.7	2.2	1.9	1.9	2.3	2.4	2.3
Al <sub>2</sub> O <sub>3</sub>	15.2	14	15	14.1	15.1	12.8	13.8	13.8
FeO	10.4	10.9	10.2	9.3	10.1	11.8	11.7	11.2
MnO	0.1	0.1	0.1	0.1	0.1	0.2	0.2	0.2
MgO	4.4	4.8	4.5	5.9	5.6	6.7	7.8	7.3
CaO	7.4	7.2	7.6	10.8	9.2	10.9	8	7.6
Na <sub>2</sub> O	4.5	4.1	5.1	4.5	5	4.4	5	5.2
K <sub>2</sub> O	1.5	1.2	0.8	1.1	1	2.1	1.8	2.2
P <sub>2</sub> O <sub>5</sub>	0.4	0.3	0.2	0.3	0.2	0.8	0.8	0.8
LOI	0.03	1.35	1	1.1	0.06	-	-	-
Total	99.13	97.85	98.3	98.1	98.16	98.2	97.7	96.2
K <sub>2</sub> O/Na <sub>2</sub> O	0.3	0.3	0.2	0.2	0.2	0.5	0.4	0.4
K <sub>2</sub> O+Na <sub>2</sub> O	6	5.3	5.9	5.6	6	6.5	6.9	7.4
Mg#	72	-	-	79	83	79	-	-
N. Neph.	0	0	1.7	9.2	7.9	15	14	16

Major element data (in wt %) are from XRF analysis. Mg # =  $100\text{Mg} / (\text{Mg} + \text{Fe}^{2+})$  calculated with  $\text{Fe}^{2+} = 0.85(\text{total Fe})$ . Total Fe reported as FeO. N. Neph= Normative nepheline, T. Ande= trachyandesite, Haw=hawaiite, Ba. T= basanite tephrite

Table 2. Ttrace elements concentrations (in ppm) of western Lut Neogene basalts.

Location	NNF					MNF		
Sample	S1-1	S1-3	S2-2	S2-3	S3-1	GM-1	GG-1	G128
Ni	90	97	91	102	111	169	173	152
Cr	131	112	153	200	232	207	217	215
V	165	157	139	142	176	217	225	215
Cs	0.5	0.6	0.5	0.3	0.6	0.6	0.9	0.8
Rb	29	35	26	21	26	49	48	45
Ba	335	455	259	219	217	466	534	539
Sr	582	646	366	647	435	904	1122	1996
Nb	37	34	21	26	21	74	80	76
Zr	208	218	169	147	129	216	220	217
Ti	16066	16327	12535	13684	11021	16274	14947	14854
Y	20	20	17	20	13	21	23	22
Hf	5.1	5.2	4.4	3.9	3.5	5.4	4.9	5
Th	1.6	1.5	2.1	1.9	1.2	4.8	6.2	5.5
U	0.6	0.5	0.4	0.6	0.4	0.6	1.8	1.6
Pb	1.9	2.9	2.2	2.1	2	DL	DL	DL
La	20.6	22.1	13.7	12.9	12.7	39.6	50.4	44.3
Ce	49.8	48.1	29.2	30.4	27.9	77.9	97.4	85.7
Pr	5.8	5.1	3.2	4	3	9	10.7	9.4
Nd	26.2	26.3	17.1	17	13.1	38.5	43.1	40.2
Sm	6.7	6.3	4.2	4.8	3.3	7.6	8.4	8.1
Eu	2.2	2.3	1.6	1.5	1.3	2.3	2.6	2.3
Gd	7	7.1	5.4	5.7	4.2	8.3	9.4	8.8
Tb	1	0.9	0.7	0.8	0.6	0.9	1	1
Yb	1.4	1.3	1.4	1.4	1.2	1.5	1.6	1.5
Lu	0.2	0.2	0.2	0.2	0.2	0.2	0.2	0.2
Zr/Nb	5.6	6.4	7.9	5.7	6.2	2.9	2.8	2.9
La/Nb	0.6	0.6	0.6	0.5	0.6	0.5	0.6	0.6
Y/Nb	0.6	0.6	0.8	0.8	0.6	0.3	0.3	0.3
(La/Yb) <sub>N</sub>	10.2	11.6	6.4	6.3	6.9	17.9	20.5	19.1

Subscript N indicates chondrite-normalized values of La and Yb. DL: Detection Limit

Table 3. Comparison of average trace elements concentration (in ppm) of western Lut Quaternary basalts with those of Tertiary-Quaternary intra-continental sodic alkali basalts and with average Oceanic Island Basalts (OIB).

Location	NNF(Lut Eastern Iran)	MNF(Lut Eastern Iran)	Arabian Peninsula (Yemen)	South Turkey		Central Anatolia (Turkey)	NW Taiwan	SE Aust.	MCAB	Av. OIB
	Age(Ma) Qt. (?)	2 - 2.6	< 1	Plio - Qt.	9.5	13 - 9	23 - 20	13	Ter. Qt.	
Ni	98	165	90	97	86	208	99	252	215	192
Cr	166	213	153	194	99	271	108	377	236	329
V	156	219	196	204	101	251	205	211	-	276
Cs	0.5	0.8	-	-	-	-	-	-	-	-
Rb	27	48	22	11	42	39	38	23	30	29
Ba	297	513	382	199	526	915	730	648	474	511
Sr	535	1341	644	673	730	932	880	765	646	718
Nb	28	77	43	29	45	77	69	62	79	52
Zr	174	218	244	144	183	331	295	216	234	255
Ti	13927	15358	-	-	-	-	-	-	-	-
Y	18	22	35	25	23	33	32	26	25	29
Hf	4	5	-	-	-	8	7	5	-	-
Th	1.7	5.5	3.9	2	9.2	9.8	5.2	7.2	6	-
U	0.5	1.3	0.8	-	-	1.7	1.1	-	-	-
Pb	2.2		2.5	13	-	-	-	-	-	-
La	16.4	44.7	33.2	20	25	64.5	50.3	39.1	38	45
Ce	37.1	87	69.6	54	49.1	128	101.5	77.9	91	94
Pr	4.2	9.7	-	-	5.2	-	-	-	-	-
Nd	19.9	40.6	34.3	-	20.6	57	52.6	37.6	42	44
Sm	5.1	8	7	-	4.5	10.7	9.8	7.6	-	-
Eu	1.8	2.4	2.3	-	1.5	-	3.1	2.3	-	-
Gd	5.9	8.8	6.8	-	4.7	-	-	-	-	-
Tb	0.8	1	-	-	-	-	-	1	-	-
Yb	1.3	1.6	2.9	-	2.1	2.1	2.2	1.7	-	-
Lu	0.2	0.2	0.4	-	0.4	0.3	0.97	0.2	-	-
Zr/Nb	6.3 2.8	5.7	4.9	4.1	4.3	4.3	3.5	3	4.9	
La/Nb	0.6	0.6	0.8	0.7	0.6	0.8	0.7	0.6	0.5	0.9
Y/Nb	0.6	0.3	0.8	0.8	0.5	0.4	0.5	0.4	0.3	0.6
(La/Yb) N	8.2	19.2	7.8	-	8.1	20.5	15.3	15.3	-	-

Data for SE Australian from [104], Yemen from [105], Central Anatolia from [35], MCAB (Massif Central alkali basalt) from [46], NW Taiwan from [36], South Turkey from [47], and average OIB from [38]. NNF: North of Nayband Fault. MNF: Middle of Nayband Fault. Qt.: Quaternary. Ter.: Tertiary

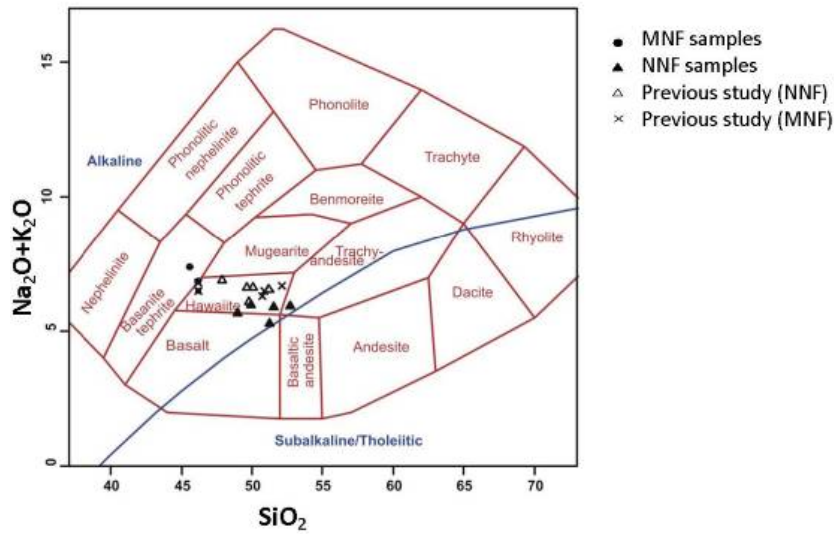


Fig. 4. Geochemical division of rocks based on  $\text{Na}_2\text{O}+\text{K}_2\text{O}$  (wt.%) against  $\text{SiO}_2$ (wt.%), from [85]. The dividing line between subalkaline and alkaline field is from [86]. Samples of previous study for NNF are taken from [28], and samples of previous study for MNF from [87].

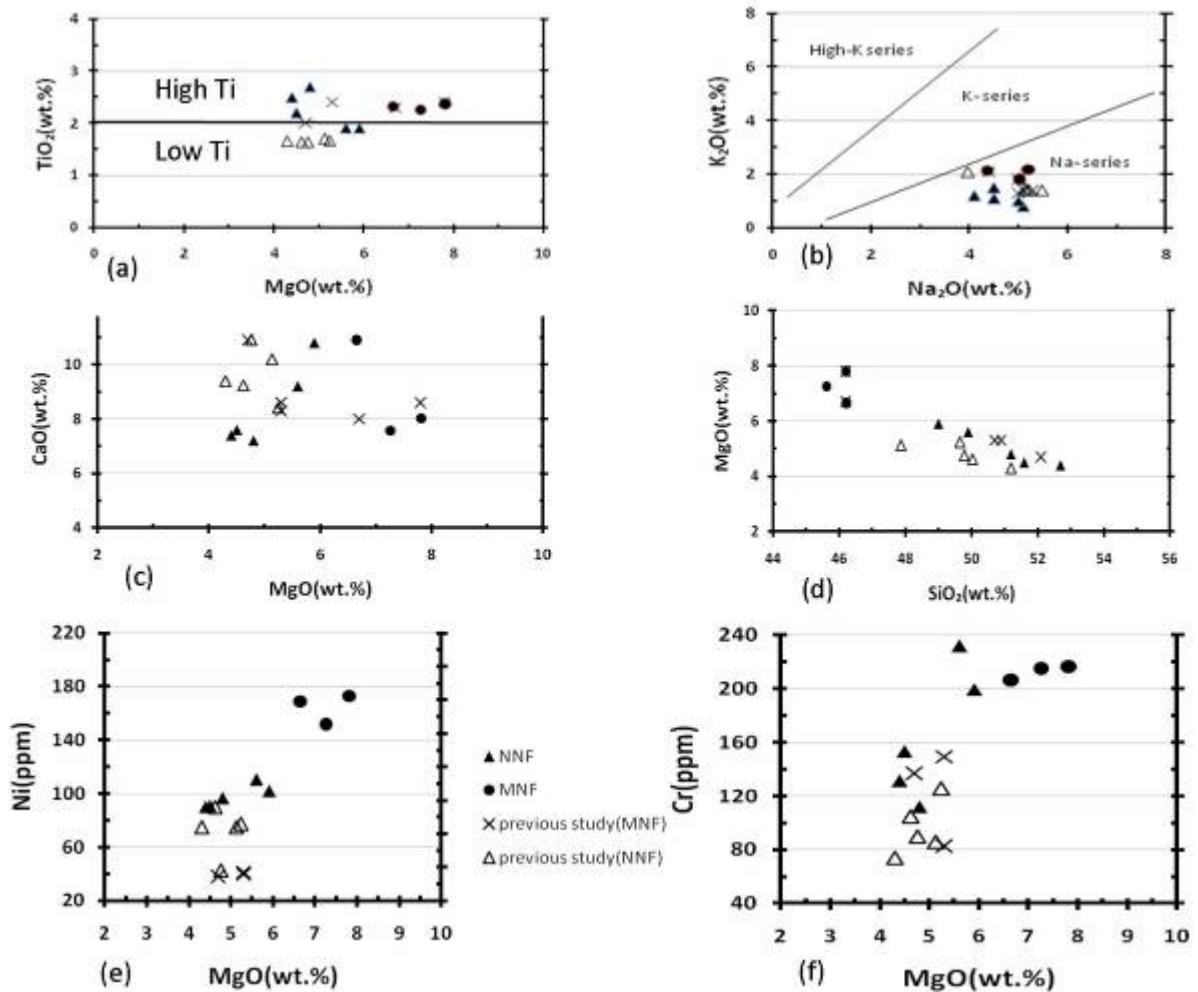


Fig. 5. (a)  $\text{TiO}_2$  versus  $\text{MgO}$  indicates that the content of Ti is high in these alkalic magma; (b)  $\text{K}_2\text{O}$  versus  $\text{Na}_2\text{O}$  diagram, showing the samples belong to the Na- series after [88]; (c) and (d) show positive  $\text{CaO}-\text{MgO}$  correlation whereas negative correlations between  $\text{SiO}_2$  contents and  $\text{MgO}$ . (e) and (f)  $\text{MgO}$  versus Ni and Cr of western Lut Neogene/Quaternary basalts.

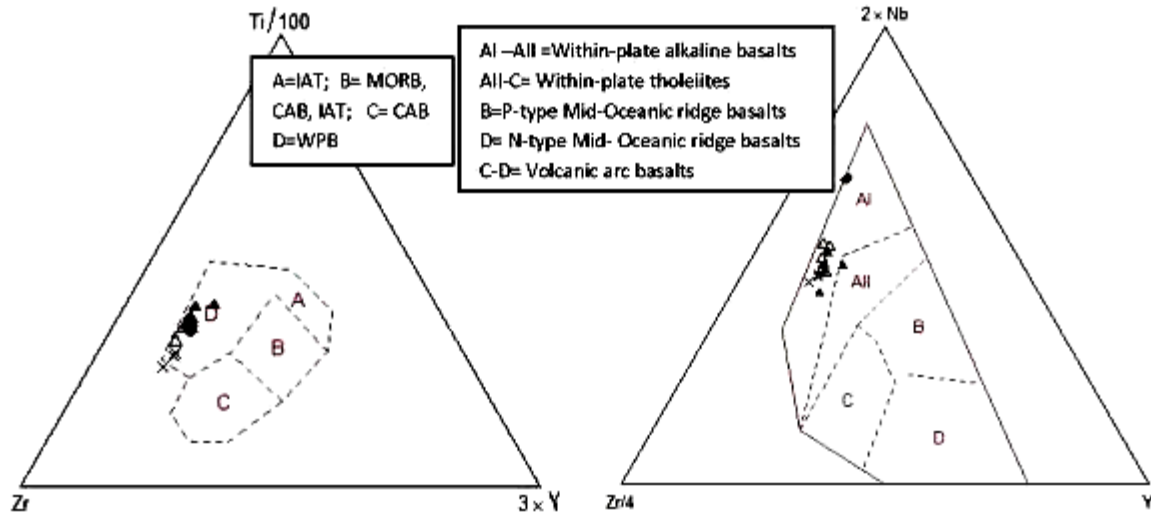


Fig. 6. Geotectonic setting based on proportions of Ti-Zr-Y [89] and Nb- Zr--Y [90]. All samples are plotted as within-plate alkaline basalts field. The symbols are the same as shown in previous figures.

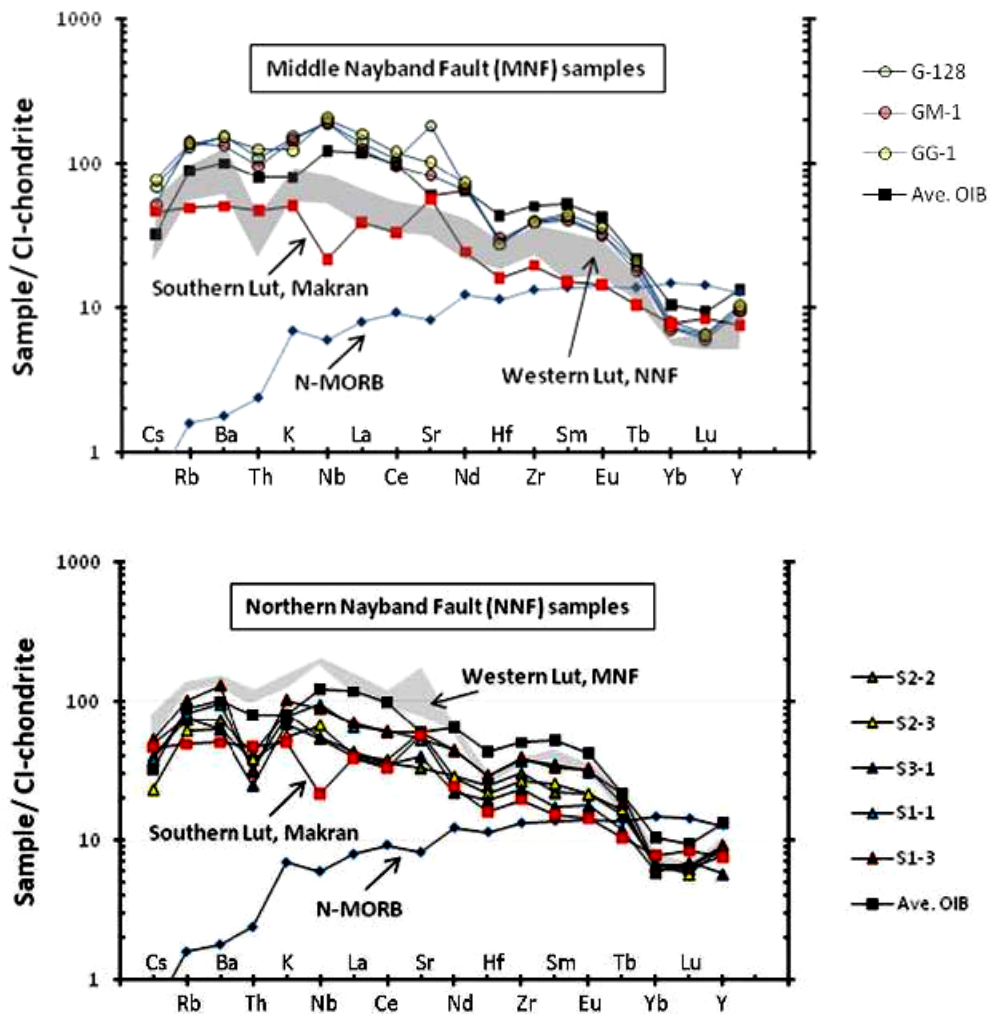


Fig. 7. Chondrite normalized multi-element for western Lut Quaternary basalts and also for average OIB and MORB, as shown in this figure, these lava show strong OIB-like characteristics. Normalization values chondrite from [91]. Average OIB from [92], MORB (N-type) from [93]and [92], average Makran arc from [60].

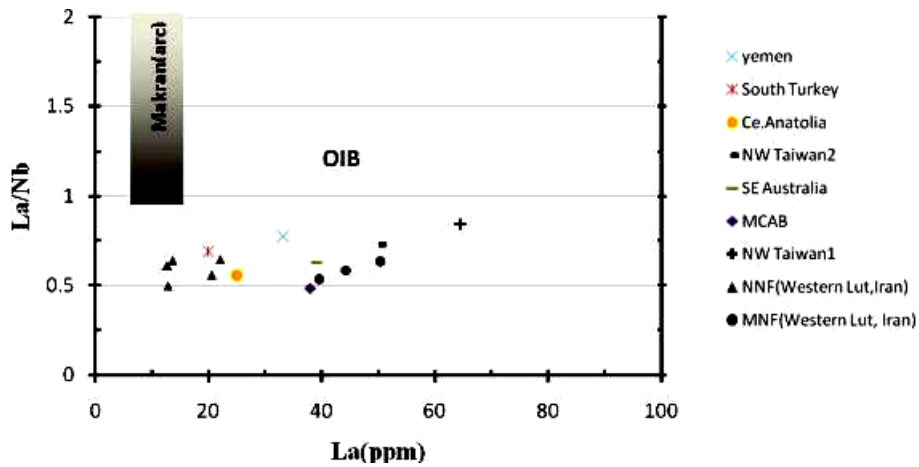


Fig. 8. La/Nb ratio versus La concentration. The limit of the field of oceanic island basalt (OIB) is taken from [94]. Makran arc from [60], the other data and abbreviation from table 3.

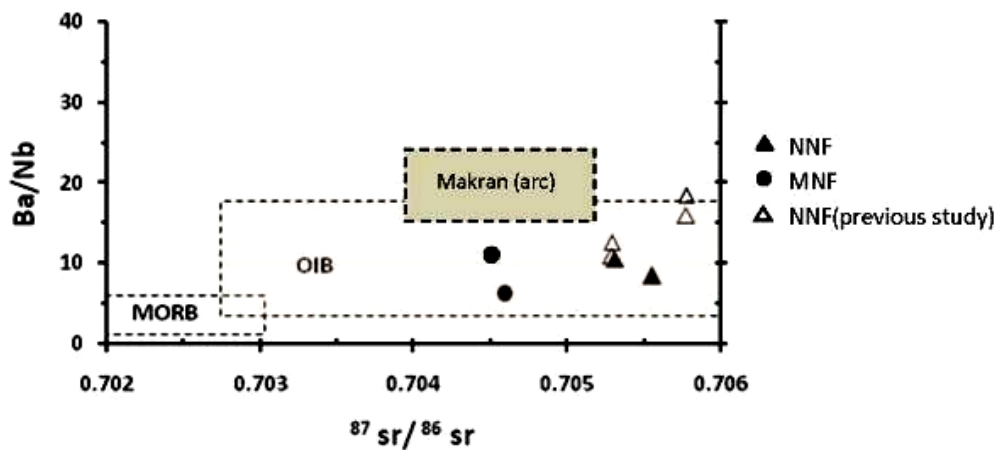


Fig. 9. Ba/Nb versus  $^{87}\text{Sr}/^{86}\text{Sr}$ . Fields for MORB and OIB from Hickey et al. (1986), Makran(arc) from [60].

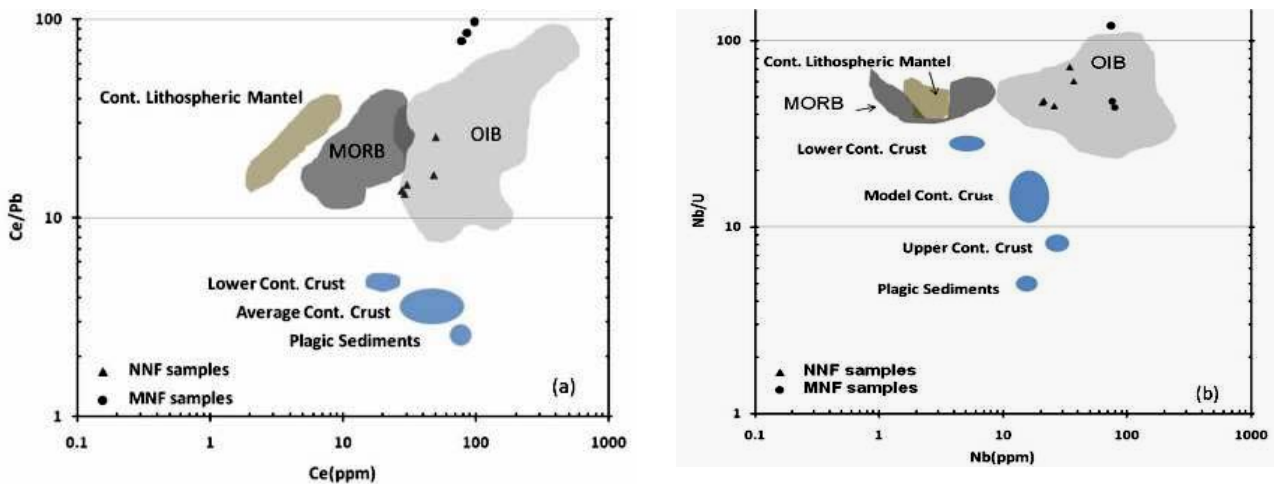


Fig. 10. (a) Ce/ Pb versus concentration of Ce and (b) Nb/U versus Nb, plotted on a log-log scale. The MORB and OIB data are taken from [95], plagic sediments from [96]. Total continental crust is taken from [43] based on the average of four models [96-99], lower continental crust [97], an estimate for the continental lithospheric mantle is taken from [100].

#### 4-4. Radiogenic isotopes

Sr–Nd–Pb isotopic ratios for western Lut Neogene basalts are given in Table 4. The  $^{87}\text{Sr}/^{86}\text{Sr}$  ratio of MNF samples ranges from 0.704505 to 0.704592 and for NNF rocks this ratio ranges from 0.705312 to 0.705555 (Table 4, Fig. 10). Hashemi et al. [28] reported that the Sr isotopic composition of four basalt and andesitic basalt from northern part of the Nayband fault (NNF) ranged from 0.705291 to 0.705777, and the newly determined values are within this range.

The Nd isotopic composition of NNF samples ranges from  $\epsilon_{\text{Nd}} = +0.94$  to  $+1.76$ , similar to four samples analyzed by Hashemi et al. (2008), which range from  $+0.91$  to  $+1.34$ . This value for MNF samples varies between  $+1.38$  to  $+1.79$  (Table 4). All samples are plotted on the right corner of the world sodic continental basalts field (Fig. 11). The Sr and Nd composition of samples from western and eastern Anatolia show different values, both with each other and also the western Lut alkali basalts (Fig. 11). The Pb isotopic composition of these alkali basalts plotted above the Northern Hemispheric Reference Line (NHRL), in the EM-2 field of OIBs (Fig. 12).

### 5. Discussion and conclusion

Based on the major and trace element compositions, the western Lut Neogene/Quaternary basalts are classified as within-plate sodic alkaline basalts (Fig. 4 and 6). These basalts have erupted along a deep crustal structure, the Nayband fault, which forms the western margin of the Lut block. To better understanding the possible causes of volcanism in this region we have to focus on determination of the mantle source characteristics and whether they are derived from the asthenosphere or from the overlying lithosphere, or a mixing of both of them [e.g., 44, 45-47].

#### 5-1. Crustal contamination

The fact that these are relatively primitive olivine-bearing alkali basalts with high Mg#, and also other geochemical features of these samples such as their La/Nb (Fig. 8), Ce/Pb and Nb/U ratios (Fig. 10), suggest that they have not been modified by crustal contamination during ascent to the surface. The  $\text{P}_2\text{O}_5/\text{K}_2\text{O}$  ratio for the MNF basalt sample is around 0.39, indicating very little contamination with crust for these younger samples from the middle part of Nayband fault (MNF). However, for the older NNF samples, this ratio is around 0.25, lower than a value of 0.4 which is considered to separate contaminated samples from uncontaminated ones [48]. The NNF basalts also have higher  $^{87}\text{Sr}/^{86}\text{Sr}$  and lower  $\epsilon_{\text{Nd}}$  than the MNF basalts, and they are associated with basaltic andesites and andesites which have even higher  $^{87}\text{Sr}/^{86}\text{Sr}$  and lower  $\epsilon_{\text{Nd}}$  indicating even greater

degrees of crustal contamination.

#### 5-2. Fractional crystallization

These samples show relatively strong positive correlation between CaO versus MgO, whereas SiO<sub>2</sub> contents show strong negative correlations with MgO that is interpreted as fractionation of olivine and clinopyroxene (Fig. 5). The compatible trace elements Ni and Cr support this observation that this magma experienced some crystal fractionation. Relatively strong positive correlation of nickel with MgO is interpreted as the presence of olivine in the fractionating assemblage (Fig. 5). The ratio of CaO/Na<sub>2</sub>O versus MgO also exhibits an excellent positive correlation (not shown) that means clinopyroxene fractionated from this magma. The positive correlation of chromium with MgO could be related to crystallization of clinopyroxene and/or a Cr-rich spinel phase. Eu has a positive correlation with SiO<sub>2</sub>, and here is no negative Eu anomaly in normalized REE patterns, indicating that fractionally crystallization did not involve plagioclase.

#### 5-3. Partial melting

According to Fitton and Dunlop [44], the trace-element composition of sodic alkali basalts, typically show evidence that their parental magma were produced by small degrees of partial melting (< 5%) of either active (plume) or passively upwelling —asthenospheric mantle. Stern et al. [49] for example described a model in which the Patagonia alkali basalts of southernmost South America are formed by relatively low degrees of partial melting of heterogeneous lower continental lithosphere and/or asthenosphere. The La/Yb ratios of the western Lut Neogene basalts increase with La concentration (Table 2), with the values of La/Yb for the younger MNF rocks (26-30) being much higher than the older NNF rocks (9-15). This increase in the La/Yb ratio could be a result of different degree of partial melting in the mantle source, different mantle sources, or both. The MNF rocks have also higher LREE and LILE abundances than NNF rocks. We suggest that the degree of partial melting may have decreased with time from north to the south along the Nayband fault. Further to the south, a very young (<1 Ma) complex of highly alkaline mafic lamproites, possibly resulting from even lower degrees of mantle melting, occurs where the Nayband fault intersects the Zargos Mountains [50].

Table 4. Sr, Nd, and Pb isotopic composition (measured) of western lut Neogene basalt.\* Data from [28]), (Ob) olivine basalt, (Ab) andesite basalt. None of the isotopic data were corrected for age.

Location	NNF						MNF	
	S2-3(Ob)	S3-1(Ob)	A-29*(Ab)	D-23*(Ob)	D-16*(Ab)	D-21*(Ob)	GM-1	GG-1
$^{87}\text{Sr}/^{86}\text{Sr}$	0.705555	0.705312	0.705774	0.705298	0.705777	0.705291	0.704592	0.704505
$^{143}\text{Nd}/^{144}\text{Nd}$	0.512728	0.512686	0.512707	0.512686	0.512709	0.512688	0.512709	0.51273
$\epsilon\text{Nd}$	1.7556	0.9363	1.34	0.94	1.32	0.91	1.385	1.794
$^{206}\text{Pb}/^{204}\text{Pb}$	18.47	18.564	-	-	-	-	18.755	18.975
$^{207}\text{Pb}/^{204}\text{Pb}$	15.556	15.581	-	-	-	-	15.583	15.596
$^{208}\text{Pb}/^{204}\text{Pb}$	38.409	38.589	-	-	-	-	38.753	38.596

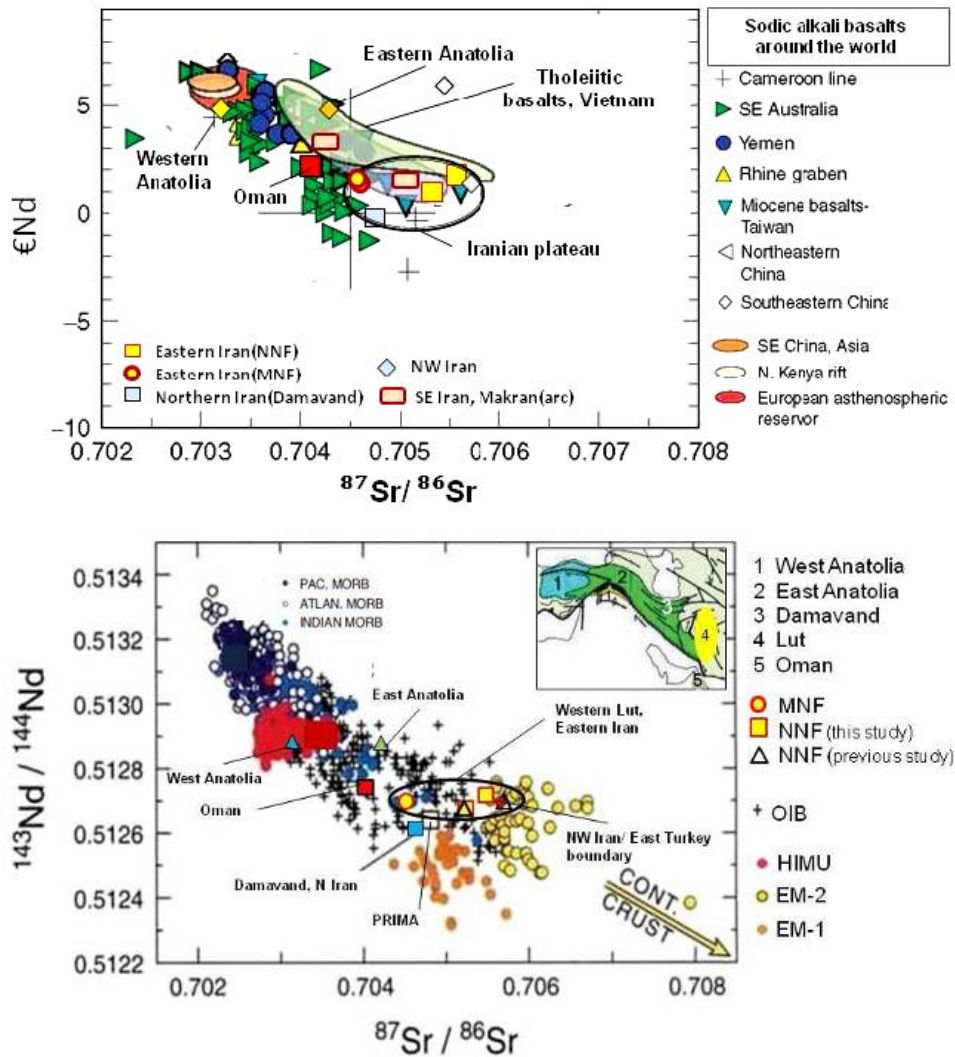


Fig. 11.  $^{143}\text{Nd}/^{144}\text{Nd}$  ratio and  $\epsilon\text{Nd}$  versus  $^{87}\text{Sr}/^{86}\text{Sr}$  comparing western Lut block samples (NNF and MNF) with the other sodic alkali basalts around the world. Top diagram from [42] and references therein, lower diagram from [55] and references therein, Sample are shown as open space triangular are taken from [28]. NWIran/East Turkey boundary from [73], Damavand from Liotard et al. [100][101], Western Anatolia from Alicic et al.[101], Eastern Anatolia from [74] and Oman from Nasir et al. [102].

#### 5-4. Primary magma characteristics and possible origin of volcanism

Although these samples do not have all the requisite features to be considered as a primary magma in equilibrium with its mantle source (i.e. Ni >400-500 ppm, Cr >1000 ppm, and high Mg values) [46, 51, 52], their contents of MgO (4.4 - 7.8 %), Mg # (68-84), Ni (90-173 ppm) and Cr (112-232 ppm) indicate that these samples crystallized from relatively primitive magma. There is no significant negative Eu anomaly which rules out fractionally crystallized plagioclase or equilibrium with a plagioclase-bearing mantle source. In addition, HREE concentration is around seven time chondrites (Fig. 7), which may suggest that garnet is absent from the source [53]. However, based on their high La/Yb values, that are between 9 to 30 and low Lu/Hf (< 0.05), the primary basaltic magma can be attributed to melting in the presence of residual garnet and therefore at least some portion of the melting must have occurred at depth below the spinel to garnet transition in mantle peridotite [51, 54-57].

The geochemical characteristics of NNF and MNF lavas show no evidence of an arc component in their source. Evidence for this includes the absence of a negative Nb anomaly relative to LREE, and low Ba/Nb (Fig. 7 and 9) and La/Nb (Fig. 8) ratios. Due to the enrichment of Nb, the values of the ratios of La/Nb versus La and Ba/Nb have an OIB signature (Figs. 8 and 9). This is consistent with the lack of evidence for subduction below this region during the Quaternary. Although the final closure of Neotethys Ocean and collision between Arabia and central Iran took place during the Neogene [58, 59], and magmatism related to northward active subduction of oceanic lithosphere of Oman Sea currently occurs beneath the Makran zone (south of the Lut block), this area presents different trace-element chemical characteristics (figs. 7-9) [60]. Both the Neotethys suture zone and the Makran magmatic arc are far (~1000 Km) away from this region. Collision between Arabia and central Iran during late Oligocene-early Miocene [61, 62] led to a transition from an extensional to a contractional tectonic regime. So, neither subduction, nor extension is documented during the last 10 Ma in this region.

Based on the  $^{87}\text{Sr}/^{86}\text{Sr}$  ratio (0.705291- 0.705777) and the value of  $^{143}\text{Nd}/^{144}\text{Nd}$  ratio (0.512686-0.512728), from NNF samples, these sodic continental basalts are plotted on OIB field and also have overlap with some EM-2 samples (Fig. 11). The  $^{87}\text{Sr}/^{86}\text{Sr}$  ratios of the samples from the middle part of the Nayband fault (MNF) are lower (0.704592-0.704505), but these sample also plots in the OIB field. Lead-isotopic compositions of all these sodic olivine basalt lavas also overlap in part of the EM-2 and OIBs field, plotted on the northern hemisphere reference line (Fig. 12).

For western and central Europe, most workers [e.g., 63,

64, 65] support models in which Tertiary and Quaternary alkalic magmatism is produced by active mantle upwelling, lithospheric extension and narrow mantle diapirs ("hot fingers") derived from a common reservoir at the base of the upper mantle. Farmer [55] suggested that the basalts with high  $\epsilon_{\text{Nd}}$  values are derived from melting of the lithospheric mantle that had been metasomatized just prior to basalt formation by incompatible element enriched fluids/melts derived from small degrees of melting of upwelling asthenosphere. Such a lithospheric mantle source has been proposed for the Yemen Quaternary sodic basalts on the Arabian Peninsula [55]. Some workers [e.g. 66, 67, 68] believe the isotope compositions and trace element enrichments of sodic alkaline magmas probably

reflect mixing of enriched lithospheric and crustal material into the asthenosphere by delamination and subduction.

Wang et al. [69] suggested that Tsaolingshan potassic magmas located in northern Taiwan mountain belt, which erupted around 0.2 Ma, formed as a result of melting dominantly of the metasomatized sub-continental lithospheric mantle (SCLM). This magma has Sr-Nd and lead isotope ratio ( $^{87}\text{Sr}/^{86}\text{Sr}=0.70540-0.70551$ ,  $^{143}\text{Nd}/^{144}\text{Nd}=0.51259-0.51268$ ,  $^{206}\text{Pb}/^{204}\text{Pb}=18.450$ ,  $^{207}\text{Pb}/^{204}\text{Pb}=15.628-15.629$  and  $^{208}\text{Pb}/^{204}\text{Pb}=38.775-38.780$ ) relatively similar to the western Lut Neogene sodic alkalic basalts, whereas the geochemical characteristics and concentration of trace and rare-earth-elements are different (see table 2 and 3 in this paper and table 2 from [69]). Chung et al. [36] proposed a binary mixing process, requiring additional involvement of an EM-2 type component, for generation the Miocene alkali basalts in northwest Taiwan. They believe this EM-2 type source, may represent either an ancient metasomatized lithospheric mantle [70] or a lower crustal granulite assemblage [71].

Barling and Goldstein [72] have tried to explain isotopic variations in Heard Island lavas, on the Kergulen Plateau, as a function of the nature of mantle reservoirs. The  $^{87}\text{Sr}/^{86}\text{Sr}$  ratios for basaltic and trachybasaltic Big Ben lavas (<1 Ma.) vary from 0.70523 to 0.70792 and  $^{143}\text{Nd}/^{144}\text{Nd}$  vary from 0.51239 to 0.51262. The ratios for Lead isotopes reported as  $^{206}\text{Pb}/^{204}\text{Pb}=17.7790-18.189$ ,  $^{207}\text{Pb}/^{204}\text{Pb}=15.551-15.566$  and  $^{208}\text{Pb}/^{204}\text{Pb}=38.646-38.358$ . The Sr- Nd and lead isotopic compositions of western Lut Neogene basalts are also close to this rang. Barling and Golstein (1990) proposed that the isotopic composition of enriched Heard component lies between that of EM1 and EM2, indicating EM components do not have distinctive isotopic composition, but rather they represent a spectrum of isotopic compositions between the most extreme composition represented by EM2 and EM1.

Finally they suggest that EM compositions reflect mantle contaminated by recycled continental crust.

Geochemical characteristics and isotopic composition of Quaternary magmatism from the Iran/Turkey borderlands (NW Iran) recently have described by Kheirkhah et al. [73]. This magmatism ranging from calc-alkali types resembling active continental margins to alkali basalts with typical within-plate characteristics [74]. The  $^{143}\text{Nd}/^{144}\text{Nd}$  values range between  $\sim 0.512627$  and  $\sim 0.512923$  ( $\text{CNd} = -2.15$  and  $+5.6$ ) and  $^{87}\text{Sr}/^{86}\text{Sr}$  ratio ranges between  $0.70461$  and  $0.705705$ . Different hypothesis are presented to describe the source regions and melting regimes of these magmatism. Pearce et al. [74] suggested lithosphere delamination as a trigger. Keskin [75] invoked break-off of the slab of Neo-Tethyan oceanic crust beneath Eurasia, especially for the concentration of magmatism in eastern Anatolia. Both mechanisms may occur [76]. The chemistry of the samples of volcanic centers in eastern Anatolia and north west Iran, with the exception of Sivas and Karacalidag, are largely derived from melting of continental lithosphere in the spine lherzolite field ( $<80$  km) and show subduction component, characterized by high La/Nb ratios and elevated LILE [73]. Pliocene–Quaternary alkali basalt flows on the Sivas pull-apart basin along the Central Anatolian Fault Zone, in eastern Anatolia have La/Nb ratios of  $\sim 1$  or  $<1$ . Melting during the strike-slip faulting and associated local extension tapped a mantle source without the regional subduction signature [73]. Parlak et al. [77] used the HREE values of Sivas volcanic center (Yb and Lu  $\sim 6$  x chondritic values) to infer melting of asthenosphere in the garnet stability field ( $>80$  km). Lavas from south of the suture at Karacalidag also have low HREE contents, and have been modelled as deriving from melts in the garnet stability field [74].

Kheirkkah et al. [73] proposed that the Sivas basalts are more confidently assigned to an asthenospheric source, similar to OIB. The cause of melting on the regional scale is related to either partial loss of the lower lithosphere, slab breakoff of Tethyan oceanic lithosphere, or a combination of the two [73].

As documented above, most of the examples of this type of magmatism around the world imply that it is not easy to provide a unique explanation to this given geochemical observations. Lut as a micro-continental block was near Arabian plate as a part of Gondwana during the early Paleozoic and it experienced different type of tectonic activities, variously rotation and laterally displacement from early Paleozoic to present. So, it is not surprising that mantle beneath the Lut block was the target of different stage of ancient and present subduction, slab breakoff, and the presence of continental crust recycled to the mantle through subduction. Low  $P_n$  velocity [78] in the Lut block and Central Iran is implying the presence of anomalously hot and/or thin mantle lid. A lithospheric delamination

event in Plio-Quaternary time may also significantly contribute to the observed widespread volcanism in this area [78]. Harig et al. [79] described that thinning of the lower lithosphere due to Rayleigh--Taylor instability can be a source for continental magmatism near active or recently active plate boundaries. They believe a mix of rheological properties could provide a mechanism for the narrow zones of thinning and upwelling, which would facilitate decompression related volcanism.

In summary, alkali olivine basalts erupted along the north and middle parts of the Nayband fault have been formed by variable (low) degrees of partial melting of similar EM-type mantle source. The degree of mantle melting may have decreased with time between 15 Ma (NNF) and 2 Ma (MNF). These low-volumes, low-degree melts rose to the surface along the very deep strike-slip Nayband fault without (MNF) or with a small amount (NNF) of interaction with the continental crust. Trace elements and isotopic composition of these lavas have been interpreted as indicating the participation of EM-type mantle asthenosphere and the continental mantle lithosphere in the generation of these magmas.

### Acknowledgment

This study is part of the first author's Ph.D. dissertation at University of Colorado, Boulder, USA. Financial support were provided by Society of Economic Geology (SEG) and the Department of Geological Sciences at CU. Special thanks to Lang Farmer and Emily Verplanck for access to TIMS lab and their help in obtaining the isotopic data for this study. We thank John Drexler for his help with electron microprobe and trace elements determination. We would like to thank to A. Malekzadeh for measuring the major elements in Ferdowsi University of Mashad (Iran). Thanks also to Paul Boni for his help and advice for preparing the thin and polish thin section. We are grateful to M. Nazemi and his friends for their field assistance in the summer of 2007 and M. Moradian, A Ghazanfari and Geological Survey of Iran, Kerman branch, for providing some samples from the study area.

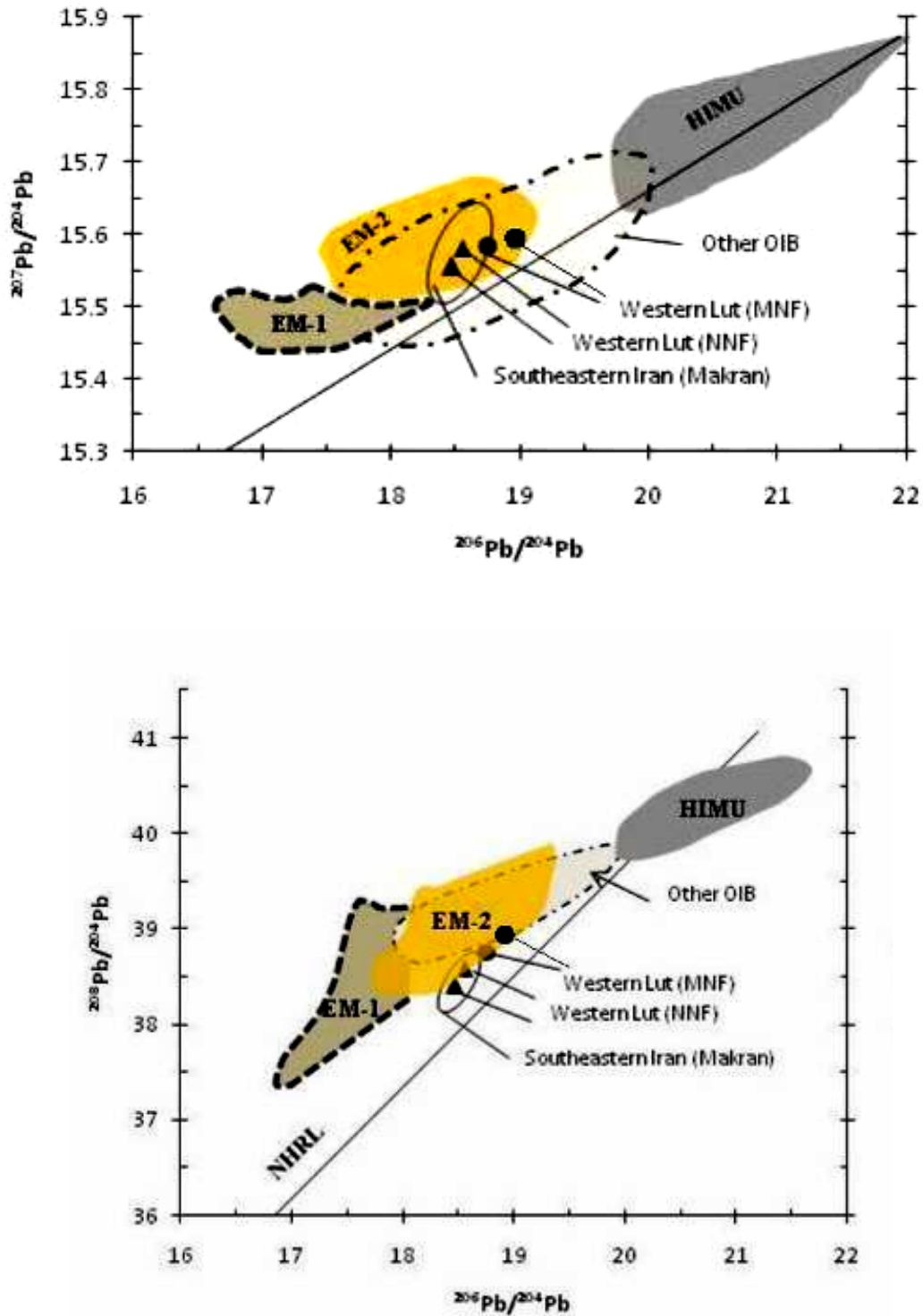


Fig. 12. Plot of  $^{207}\text{Pb}/^{204}\text{Pb}$  and  $^{208}\text{Pb}/^{204}\text{Pb}$  versus  $^{206}\text{Pb}/^{204}\text{Pb}$ . Source of data and filed similar to figure 10. NHRL= Northern Hemisphere Reference Line [103].

**References**

[1] Jung, D., J. Keller, R. Khorasani, C. Marcks, A. Baumann, and P. Horn, 1984, Petrology of the Tertiary magmatic activity in the northern Lut area, east Iran:

Neues Jahrbuch für Geologie und Palaontologie Abhandlungen, v. 160, p. 417-467.  
 [2] Conrad, G., R. Montignary, R. Thuizat, and M. Westphal, 1981, Tertiary and Quaternary geodynamics of southern

- Lut (Iran) as deduced from palaeomagnetic, isotopic and structural data: *Tectonophysics*, v. 75, p. T11-T17.
- [3] Walker, R. T., P. Gans, M. B. Allen, J. Jackson, M. Khatib, N. Marsh, and M. Zarrinkoub, 2009, Late Cenozoic volcanism and rates of active faulting in eastern Iran: *Geophys. J. Int.*, v. 177, p. 783-805.
- [4] Shafiei, B., M. Haschke, and J. Shahabpour, 2009, Recycling of orogenic arc crust triggers porphyry Cu mineralization in Kerman Cenozoic arc rocks, southeastern Iran: *Miner Deposita*, v. 44, p. 265-283.
- [5] Stöcklin, J., 1968, Structural history and tectonics of Iran: a review: *American Association of Petroleum Geology Bulletin*, v. 52, p. 1229-1258.
- [6] Mohajer-Ashjai, H., H. Behzadi, and M. Berberian, 1975, Reflection on the rigidity of the Lut block and recent crustal deformation in eastern Iran: *Tectonophysics*, v. 25, p. 281-301.
- [7] Haghypour, A., 1981, Precambrian in central Iran: lithostratigraphy, structural history and petrology: *Iranian Petroleum Institute Bulletin*, v. 81, p. 1-17.
- [8] Nadimi, A., 2007, Evolution of central Iranian basement: *Gondwana Research*, v. 12, p. 324-333.
- [9] Davoudzadeh, M., 1997, *Encyclopedia of European and Asian regional geology*, p. 384-405.
- [10] Samani, B., C. Zhuyi, G. Xuetao, and T. Chuan, 1994, Geochemistry of Quaternary Olivine Basalts From the Lut Block, Eastern Iran: *Geosciences Quarterly*, v. 3, p. 40-63.
- [11] Hassanzadeh, J., S. F. Daniel, H. K. Brian, A. J. Gary, S. D. Lisa, G. Marty, S. K. Axel, and W. J. Douglas, 2008, U-Pb zircon geochronology of late Neoproterozoic-Early Cambrian granitoids in Iran: Implications for paleogeography, magmatism, and exhumation history of Iranian basement: *Tectonophysics*, v. 451, p. 71-96.
- [12] Stöcklin, J., J. Eftekhamejad, and A. Hoshmandzadeh, 1971, Initial investigation of central Lut block, eastern Iran, *Geological Survey of Iran*, p. 88.
- [13] Esmaily, D., A. Nédélec, M. V. Valizadeh, F. Moore, and J. Cotton, 2005, Petrology of the Jurassic Shah-Kuh granite (eastern Iran), with reference to tin mineralization: *Asian Earth Sciences*, v. 25, p. 961-980.
- [14] Lensch, G., and K. Schmidt, 1984, Plate tectonic, orogeny, and mineralization in the Iranian fold belts: *Geol. Palaont.*, v. 168, p. 558-568.
- [15] Zarrinkoub, M. H., S. L. Chung, S. S. Mohamadi, and M. M. Khatib, 2008, Age dating, petrography and geochemistry of Fanoud volcanic rocks (South east of Birjand, Iran): 16th Iranian Society of Crystallography & Mineralogy, Iran.
- [16] Moinvaziri, H., and E. Aminshobhani, 1978, Etudes volcanologique du Taftan. Ecole normale superieure de Tehran.
- [17] Ghazban, F., 2004, Alteration and geochemistry of Mount Taftan geothermal prospect southeastern Iran: *Iranian International Journal of Science*, v. 5, p. 43-62.
- [18] Stöcklin, J., E. J., Hoshmandzadeh, A., 1972, Geological reconnaissance map of Central Lut, Geological Survey of Iran.
- [19] Arjangraves, B., 1972, Investigation on geology and petrology of volcanic rocks in south of Birjand, Sahl Abad area, south east of Iran, University of Tehran, Tehran, Iran.
- [20] Emami, M. H., 1972, Geology and petrological investigation on Shahkuh volcanic rocks, south of Birjand, eastern Iran, University of Tehran, Tehran, Iran.
- [21] Darvishzadeh, A., E. M. Moores, and R. W. Fairbridge, 1976, Les caractères du volcanisme tertiaire de East Iranian-block du Lut: *Cahiers géologiques*, v. 92, p. 147-151.
- [22] Rosenberg, F., 1981, Geochemische und petrologische Untersuchungen and magmatiten und kontaktmetamophen Rahmen-gnsteineh Intrusion Bejestan, Ostiran- Diplomarbeit: Mir. Petr. Inst Hamburg, p. 133.
- [23] Khorasani, R., 1982, Petrographie und Gechemie spatkreuzisch, alttertiärer Laven und subvolnrite der nordichen Lut, Universität Hambur, in Vorbereitung.
- [24] Vosughi Abedini, M., 1997, Petrologic and tectono magmatic aspects of Cenozoic basalts in Iran (Khorasan): *Earth Science Journal*, v. 23-24, p. 16-30.
- [25] Ghorbani, G., 1997, Petro genetic studies of Eastern Iran Quaternary Basalts (Khorasan), Shahid Beheshti University, Tehran, Iran, 192 p.
- [26] Allahpoor, E., 1997, Investigation of petrogenesis and geochemistry of Tertiary volcanism in north of Birjand with special aspect to mineralization, University of Shahid Beheshti, Tehran, Iran.
- [27] Hashemi, S. M., 1997, Petrology, geochemistry studies of volcanic Shotori Mountain (east of Tabas), Shahid Beheshti University, Tehran, Iran.
- [28] Hashemi, S. M., M. Emami, M. Vossoughi Abedini, M. Pourmoafi, and M. Ghorbani, 2008, Petrology of Quaternary Basalts of Tabas (East of Iran): *Earth Science*, v. 68, p. 26-39.
- [29] Pourlatifi, A., 2002, Investigation on petrology of Eocene volcanic rocks in Ferdows quadrangle geological map, (south of Khorasan): Petrology thesis, Tehran, Iran.
- [30] Boomeri, M., 2004, Geochemistry, petrography and formation style of Taftan Volcano, Research Project Report, University of Sistan & Baluchistan, Iran, p. p. 118.
- [31] Reed, S. J. B., 1996, *Electron Microscope Analysis and Scanning Electron Microscopy in Geology*: Cambridge University Press, p. 201.
- [32] Briggs, P., 1996, The determination of forty elements in geological materials by inductively coupled plasma-atomic: Bf Arbogast, U.S: Geological Survey, p. 77-94.
- [33] Farmer, G. L., E. D. Broxton, W. G. R., and W. Pickthon, 1991, Nd, Sr, and O isotopic variations in metaluminous ash-flow tuffs and related volcanic rocks at Timber Mountain/ Oasis Valley Caldera, Complex, Sw Nevada: implication for the origion and evolution of large-volume silicic magma bodies: *Contributions to Mineralogy and Petrology*, v. 109, p. 53-68.
- [34] Farmer, G. L., A. F. Glazner, and C. R. Manley, 2002, Did lithospheric delamination trigger late Cenozoic potassic volcanism in the southern Sierra Nevada, California: *GSA Bulletin*, v. 114, p. 754-768.
- [35] Wilson, M., A. Tankurt, and N. Gulec, 1997, Tertiary volcanism of the Galatia province, north-west Central Anatolia, Turkey: *Lithos*, v. 42, p. 105-122.
- [36] Chnug, S.-L., B.-M. Jahn, S.-J. Chen, L. Typhoon, and C.-H. Chen, 1995, Miocene basalts in northwestern Taiwan: Evidence for EM-type mantle sources in the continental lithosphere: *Geochimica et Cosmochimica Acta*, v. 59, p. 549-55.
- [37] Allegre, C. J., and D. L. Turcotte, 1985, Geodynamic mixing in the mesosphere boundary layer and the origin

- of oceanic islands: *Geophysics Research Letter*, v. 12, p. 207-210.
- [38] Fitton, J. G., J. Dodie, and W. P. Leeman, 1991, Basic magmatism associated with late Cenozoic extension in the Western United States: compositional variations in space and time.: *Geophys*, v. 96, p. 13693-13711.
- [39] Menzies, M. A., and P. R. Kyle, 1991, Continental volcanism: a crust-mantle probe. In: *Continental Mantle: Oxford Monographs on Geology and Geophysics*, p. 157-177.
- [40] Thompson, R. N., and M. A. Morrison, 1988, Asthenospheric and lower lithospheric mantle contributions to continental extensional magmatism: an example from the British Tertiary Province: *Chem. Geol*, v. 68, p. 1-15.
- [41] Sun, S. S., and M. F. McDonough, 1989, In *Magmatism in the Ocean Basins: special Publication of the Geological Society*, v. 42, p. 313-345.
- [42] Hofmann, A. W., 1997, Mantle geochemistry: the message from oceanic magmatism: *Nature*, v. 385, p. 219-229.
- [43] Sims, K.W.W., DePaolo, D.J., 1997, Inferences about mantle magma sources from incompatible element concentration ratios in oceanic basalts, *Geochemica et cosmochimica Acta* 61, No. 4, p. 765-784.
- [44] Fitton, J. G., and H. M. Dunlop, 1985, the Cameroon Line, West Africa, and its bearing on the origin of oceanic and continental alkali basalt: *Earth and Planetary Science Letters*, v. 72, p. 23-38.
- [45] Weaver, B. L., D. A. Wood, J. Tarney, and J. L. Joron, 1987, Geochemistry of ocean island basalts from the South Atlantic Ocean: Ascension, Bouvet, St. Helena, Gough and Tristan da Cunha. In: Fitton, J.G. and Upton, B.G.J., Editors, 1987. *Alkaline Igneous Rocks: Geological Society of London Special Publication*, v. 30, p. 253-267.
- [46] Wilson, M., and H. Downes, 1991, Tertiary-Quaternary extension-related alkaline magmatism in western and central Europe: *Petrology*, v. 32, p. 811-849.
- [47] Yurtmen, S., G. Rowbotham, F. ler, and P. A. Floyd, 2000, Petrogenesis of Basalts from Southern Turkey: the Plio-Quaternary Volcanism to the North of skenderun Gulf: *Geological Society, London, Special Publications*, v. v. 173, p. pp. 489-512.
- [48] Miller, J.S., Glazner, A.F., Farmer, G.L., Suayah, I.B., Ketien, L.A., 2000, A Sr, Nd, and Pb isotopic study of mantle domains and crustal structure from Miocene volcanic rocks in the Mojave Desert, California, *GSA Bulletin*, v. 112; no. 8, p. 1264-1279.
- [49] Stern, C. R., F. A. Frey, K. Futa, R. E. Zartman, Z. Peng, and T. K. Kyser, 1990, Trace element and Sr, Nd, Pb and O isotopic composition of Pliocene and Quaternary alkali basalts of the Patagonian plateau lavas of southernmost South America: *Contributions to Mineralogy and Petrology*, v. 104, p. 294-308.
- [50] Saadat, S., C. R. Stern, and M. H. Karimpour, 2009, Quaternary mafic volcanic rocks along the Nayband fault, Lut block, eastern Iran: *GSA Annual meeting*, p. 480.
- [51] Frey, F. A., D. H. Green, and S. D. Roy, 1978, Integrated models of basalt petrogenesis: a study of quartz tholeiites to olivine melilitites from southeastern Australia utilizing geochemical and experimental petrologic data: *Journal of Petrology*, v. 19, p. 463-513.
- [52] Winter, J. D., 2001, *An Introduction to Igneous and Metamorphic Petrology*. NJ: Prentice Hall, Upper Saddle River, Prentice- Hall Inc., 697 p.
- [53] Wilson, M., 1989, *Igneous petrogenesis: a global tectonic approach*: Unwin Hyman, p. 466.
- [54] Beard, B. L., and C. M. Johnson, 1997, Hafnium isotope evidence for the origin of Cenozoic basaltic lavas from the southwestern United States: *Journal of Geophysical Research*, v. 102, p. 20149-20178.
- [55] Farmer, G. L., 2003, *Continental basaltic rocks: Treatise on Geochemistry*, v. 3, p. 1-39.
- [56] Langmuir, C. H., E. M. Klein, and T. Plank, 1992, Petrological systematics of mid-ocean ridge basalts: constraints on melt generation beneath ocean ridges: *Geophysical Monograph* 71, American Geophysical Union, p. 183-280.
- [57] Thirlwall, M. F., U. B. G. J., and c. Jenkins, 1994, Interaction between continental lithosphere and the Iceland Plume Sr-Nd-Pb isotope geochemistry of Tertiary basalts, NE Greenland: *J. Petrol.*, v. 35, p. 839-879.
- [58] Berberian, F., and M. Berberian, 1982, Tectono-plutonic episodes in Iran. In: (Gupta, H.K. and Delaney, F.M., eds) *Zagros, Hindu Kush, Himalaya Geodynamic Evolution: American Geophysical Union, geodynamics series*, v. 03, p. 5-32.
- [59] Berberian, M., and G. C. P. King, 1981, Towards a paleogeography and tectonic evolution of Iran: *Canadian Journal of Earth Sciences*, v. 18, p. 210-265.
- [60] Saadat, S., C. R. Stern, and M. H. Karimpour, 2008, Geochemistry of Quaternary Olivine Basalts From the Lut Block, Eastern Iran, AGU Fall meeting, San Francisco, California.
- [61] Fakhari, M. D., G. J. Axen, B. K. Horton, J. Hassanzadeh, and A. Amini, 2008, Revised age of proximal deposits in the Zagros foreland basin and implications for Cenozoic evolution of the High Zagros: *Tectonophysics*, v. 451, p. 170-185.
- [62] Horton, B. K., J. Hassanzadeh, D. F. Stockli, G. J. Axen, R. J. Gillis, B. Guest, A. H. Amini, M. Fakhari, S. M. Zamanzadeh, and M. Grove, 2008, Detrital zircon provenance of Neoproterozoic to Cenozoic deposits in Iran: Implications for chronostratigraphy and collisional tectonics: *Tectonophysics*, v. 451, p. 97-122.
- [63] Oyarzun, R., M. Doblas, J. Lopez-Ruiz, and J. M. Cebria, 1997, Opening of the central Atlantic and asymmetric mantle upwelling phenomena: implications for long-lived magmatism in western North Africa and Europe: *Geology*, v. 25, p. 727-730.
- [64] Wedepohl, K. H., and A. Baumann, 1999, Central European Cenozoic plume volcanism with OIB characteristics and indications of a lower mantle source: *Contrib. Mineral. Petrol.*, v. 136.
- [65] Wilson, M., and R. Patterson, 2001, Intraplate magmatism related to short-wavelength convective instabilities in the upper mantle: evidence from the Tertiary- Quaternary volcanic province of western and central Europe. In *Mantle Plumes: Their Identification through Time: Geological Society of America Special Papers*, v. 352, p. 37-58.
- [66] Hart, S. R., 1988, Heterogeneous mantle domains: signatures, genesis and mixing chronologies, *Earth Planet: Science*, v. 90, p. 273-296.
- [67] McKenzie, D., and R. K. O'Nions, 1983, Mantle reservoirs and ocean island basalts: *Nature*, v. 301, p.

- 229-231.
- [68] White, W. M., and A. W. Hofmann, 1982, Sr and Nd isotope geochemistry of oceanic basalts and mantle evolution: *Nature*, v. 294, p. 821-825.
- [69] Wang, K. L., S. L. Chung, S. Y. O'Reilly, S. S. Sun, R. Shinjo, and C. H. Chen, 2004, Geochemical Constraints for the Genesis of Post-collisional Magmatism and the Geodynamic Evolution of the Northern Taiwan Region: *Petrology*, v. 45, p. 975-1011.
- [70] Menzies, M. A., N. Rogers, A. Tindle, and C. J. Hawesworth, 1987, Metasomatic and enrichment processes in lithospheric peridotites: an effect of asthenosphere-lithosphere interaction. In *Mantle Metasomatism*: Academic Press (1987), p. 313-361.
- [71] Ben Othman, D., M. Polve, and C. J. Allegre, 1984, Nd-Sr isotopic composition of granulites and constrains on the evolution of the lower continental crust: *Nature*, v. 307, p. 510-515.
- [72] Barling, J., and S. L. Goldstein, 1990, Extreme isotopic variations in Heard Island lavas and the nature of mantle reservoirs: *Nature*, v. 348(6296), p. 59-62.
- [73] Kheirkhah, M., M. B. Allen, and M. Emami, 2009, Quaternary syn-collision magmatism from the Iran/Turkey borderlands: *Journal of Volcanology and Geothermal Research*, v. 182, p. 1-12.
- [74] Pearce, J. A., J. F. Bender, S. E. De Long, W. S. F. Kidd, P. J. Low, Y. Gijner, F. Saroglu, Y. Yilmaz, S. Moorbatg, and J. G. Mitchell, 1990, Genesis of collision volcanism in Eastern Anatolia, Turkey: *Journal of Volcanology and Geothermal Research*, v. 44, p. 189-229.
- [75] Keskin, M., 2003, Magma generation by slab steepening and breakoff beneath a subduction-accretion complex: An alternative model for collision-related volcanism in Eastern Anatolia, Turkey: *Geophysical Research Letters*, v. 30, p. 1-4.
- [76] Keskin, M., 2007, Eastern Anatolia: a hot spot in a collision zone without a mantle plume. In: G.R. Foulger and D.M. Jurdy, Editors, *Plates, Plumes, and Planetary Processes*: Geological Society of America, p. 1-25.
- [77] Parlak, O., M. Delaloye, C. Demirkol, and U. C. Unlugenc, 2001, Geochemistry of Pliocene/ Pleistocene basalts along the Central Anatolian Fault Zone (CAFZ), Turkey: *Geodinamica Acta*, v. 14, p. 159-167.
- [78] Al-Lazki, A. I., E. Sandvol, D. Seber, M. Barazangi, T. N., and R. Mohamad, 2004, Pn tomographic imaging of mantle lid velocity and anisotropy at the junction of the Arabian, Eurasian, and African plates: *Geophysical Journal International*, v. 158, p. 1024-040.
- [79] Harig, C., P. Molnar, and G. Houseman, 2010, Thinning and Localization of Deformation During Rayleigh-Taylor Instability and its Implication for Intracontinental Magmatism: *Journal of Geophysical Research*, v. 115, p. 11.
- [80] Bird, P., 2003, An updated digital model of plate boundaries: *Geochemistry, Geophysics, Geosystems*, v. 4(3)1027, doi:10.1029/2001GC000252.
- [81] Alavi, M., 1991, Sedimentary and structural characteristics of the Paleo-Tethys remnants in northeastern Iran: *Geological Society of America Bulletin*, v. 103, p. 983-992.
- [82] Natalin, B. A., and A. M. C. Sengor, 2005, Late Palaeozoic to Triassic evolution of the Turan and Scythian platforms: The pre-history of the Palaeo-Tethyan closure: *Tectonophysics*, v. 404, p. 175-202.
- [83] Nilforoushan, F., F. Masson, P. Vernant, C. Vigny, J. Martinod, M. Abbassi, H. Nankali, D. Hatzfeld, R. Bayer, F. Tavakoli, A. Ashtiani, E. Doerflinger, M. Daignie' res, P. Collard, and J. Che'ry, 2003, GPS network monitors the Arabia-Eurasia collision deformation in Iran: *Journal of Geodesy*, v. 77, p. 411-422.
- [84] De Mets, C., R. G. Gordon, D. F. Argus, and S. Stein, 1990, Current plate motions: *Geophys. J. Int.*, v. 101, p. 425-478.
- [85] Cox, K. G., J. D. Bell, and R. J. Pankhurst, 1979, *The Interpretation of Igneous Rocks*: London, George Allen and Unwin, 445 p.
- [86] Myashiro, A., 1978, Nature of Alkalic volcanic rock series: *Contributions to Mineralogy and Petrology*, v. 66, p. 91-104.
- [87] Girod, M., Conrad, G., 1975, Les formations volcaniques récentes du Sud de l'Iran (Kouh-e-Shahsavaran); données pétrologiques préliminaires; implications structurales, *Bull. Volcanol.* v. 39, p. 1-17.
- [88] Middlemost, E. A. K., 1975, The basalt clan: *Earthscience Rev.*, v. 11, p. 337-364.
- [89] Pearce, J. A., and J. R. Cann, 1973, Tectonic setting of basic volcanic rocks determined using trace element analyses: *Earth and Planetary Science Letters*, v. 19, p. 290-300.
- [90] Meschede, M., 1986, A method of discriminating between different types of mid-ocean ridge basalts and continental tholeiites with the Nb-Zr-Y diagram: *Chem Geol*, v. 56, p. 207-218.
- [91] Gerlach, D., F. A. Frey, H. Moreno-Roa, and L.-E. L., 1988, Recent volcanism in the Puheyue-Cordon Caulle region, southern Andes, Chile(40.5 degree S); Petrogenesis of evolved lavas: *Journal of Petrol*, v. 29, p. 332-382.
- [92] Sun, S. S., 1980, Lead isotopic study of young volcanogenic rocks from mid-ocean ridges, ocean islands and island arcs: *Philosophical Transactions of the Royal Society of London*, p. 409-445.
- [93] Saunders, A. D., and J. Tarney, 1984, Geochemical characteristics of basaltic volcanism within back-arc basins. In: Kokelaar, B. P. & Howells, M. F. (eds) *Marginal Basin Geology Volcanic and associated sedimentary and tectonic processes in modern and ancient marginal basins*: Special Publication of the Geological Society, p. 59-76.
- [94] Hickey, R. L., F. A. Frey, D. C. Gerlach, and L. López-Escobar, 1986, Multiple sources for basaltic arc rocks from the Southern Volcanic Zone of the Andes (34°-41°S): Trace element and isotopic evidence for contributions from subducted oceanic crust, mantle and continental crust: *Journal of Geophysical Research*, v. 91, p. 5963-5983.
- [95] Hofmann, A. W., K. P. Jochum, M. Seufert, and W. M. White, 1986, Nb and Pb in oceanic basalts: new constraints on mantle evolution: *Earth and Planetary Science Letters*, v. 79, p. 33-45.
- [96] Taylor, S. R., and S. M. McLennan, 1985, *The continental crust: Its composition and evolution*, Blackwell Scientific Publications, p. 312.
- [97] Rudnick, R. L., and D. M. Fountain, 1995, Nature and composition of the continental crust: a lower crustal perspective: *Geophys.*, v. 33, p. 267-309.
- [98] Weaver, B. L., and J. Tarney, 1984, Empirical approach

- to estimating the composition of the continental crust: *Nature*, v. 310, p. 575-577.
- [99] Wedepohl, K. H., 1994, The composition of the continental crust(abstract): *Mineral. Mag.*, v. 58, p. 359-360.
- [100] Liotard, J. M., J. M. Dautria, B. D, M. Condomines, H. Mehdizadeh, and J. F. Ritz, 2008, Origin of the absarokite-banakitite association of the Damavand volcano (Iran): trace elements and Sr, Nd, Pb isotope constraints: *Int. J. Earth Sci (Geol Rundsch)*, v. 97, p. 89-102.
- [101] Alicic, P., A. Temel, and A. Gourgaud, 2002, Pb-Nd-Sr isotope and trace element geochemistry of Quaternary extension-related alkaline volcanism: a case study of Kula region (western Anatolia, Turkey): *Journal of Volcanology and Geothermal Research*, v. 115, p. 487-510.
- [102] Nasir, S., A. Al-Sayigh, A. Alharthy, and A. Al-Lazki, 2006, Geochemistry and petrology of Tertiary volcanic rocks and related ultramafic xenoliths from the central and eastern Oman Mountains: *Lithos*, v. 90, p. 249-270.
- [103] Hart, S. R., 1984, A large-scale isotope anomaly in the Southern Hemisphere mantle: *Nature*, v. 309, p. 753-757.
- [104] Zhang, M., and S. Y. O'Reilly, 1997, Multiple sources for basaltic rocks from Dubbo, eastern Australia: geochemical evidence for plume-lithosphere interaction: *Chem Geol*, v. 136, p. 33-54.
- [105] Baker, J. A., M. A. Menzies, M. F. Hirlwall, and C. G. MacPherson, 1997, Petrogenesis of Quaternary Intraplate Volcanism, Sana'a, Yemen: Implications for Plume-Lithosphere Interaction and Polybaric Melt Hybridization: *Journal of Petrology*, v. 38, p. 1359-1390.